- Avasimibe lowers body weight and body fat in high-fat diet-induced obese mice
- Avasimibe ameliorates systemic glucose homeostasis in obese mice
- Avasimibe-induced body weight loss in obese mice is largely attributed to the suppression of food intake

# Pharmacological inhibition of acyl-coenzyme A:cholesterol acyltransferase alleviates obesity and insulin resistance in diet-induced obese mice by regulating food intake

Yuyan Zhu[1,2,*], Sora Q. Kim[3], Yuan Zhang[4], Qing Liu[2], Kee-Hong Kim[1,5,6*]

From the [1]Department of Food Science, [3]Department of Nutrition Science, [5]Purdue Center for Cancer Research, [6]Purdue Institute for Drug Discovery, Purdue University, West Lafayette, IN 47907, USA

[2]Department of Applied Biology and Chemical Technology, Hong Kong Polytechnic University, Hung Hom, Hong Kong, China

[4]College of Food Science, Southwest University, Chongqing, 400715, China

Running Title: A Therapeutic Potential of Avasimibe for Obesity

[*] Correspondence:

Kee-Hong Kim; Department of Food Science, Purdue University, West Lafayette, IN 47907; E-mail: keehong@purdue.edu, Tel.: +1-765-496-2330

Yuyan Zhu; Department of Applied Biology and Chemical Technology, Hong Kong Polytechnic University, Hung Hom, Hong Kong, China; E-mail: yuyan.zhu@polyu.edu.hk, Tel: +852-3400-8678

**Abstract**

**Background/Objectives:** Acyl-coenzyme A:cholesterol acyltransferases (ACATs) catalyze the formation of cholesteryl ester (CE) from free cholesterol to regulate intracellular cholesterol homeostasis. Despite the well-documented role of ACATs in hypercholesterolemia and their emerging role in cancer and Alzheimer's disease, the role of ACATs in adipose lipid metabolism and obesity is poorly understood. Herein, we investigated the therapeutic potential of pharmacological inhibition of ACATs in obesity.

**Methods:** We administrated avasimibe, an ACAT inhibitor, or vehicle to high-fat diet-induced obese (DIO) mice via intraperitoneal injection and evaluated adiposity, food intake, energy expenditure, and glucose homeostasis. Moreover, we examined the effect of avasimibe on the expressions of the genes in adipogenesis, lipogenesis, inflammation and adipose pathology in adipose tissue by real-time PCR. We also performed a pair feeding study to determine the mechanism for body weight lowering effect of avasimibe.

**Results:** Avasimibe treatment markedly decreased body weight, body fat content and food intake with increased energy expenditure in DIO mice. Avasimibe treatment significantly lowered blood levels of glucose and insulin, and improved glucose tolerance in obese mice. The beneficial effects of avasimibe were associated with lower levels of adipocyte-specific genes in adipose tissue and the suppression of food intake. Using a par-feeding study, we further demonstrated that avasimibe-promoted weight loss is attributed mainly to the reduction of food intake.

**Conclusions:** These results indicate that avasimibe ameliorates obesity and its-related insulin resistance in DIO mice through, at least in part, suppression of food intake.

**Keywords:** acyl-coenzyme A: cholesterol acyltransferase, cholesterol ester, avasimibe, obesity, insulin resistance, food intake

**Abbreviations:**

ACATs, Acyl-coenzyme A:cholesterol acyltransferases; CE, cholesterol ester; DIO, diet-induced obese; TG, triglyceride; LD, lipid droplet; FC, free cholesterol; epiWAT, epididymal white adipose tissue; VLDL, very low-density lipoprotein; AVA, avasimibe; CTRL, control; ALT, alanine transaminase; IPGTT, Intraperitoneal glucose tolerance test; HOMA-IR, homeostatic model assessment of insulin resistance; HF, high fat; RER, respiratory exchange ratio.

## 1. Introduction

Obesity is drawing increasing attention due to its high global prevalence, increased metabolic health risks and heavy economic burden. Obesity is characterized by an excess of adipose tissue due to the massive accumulation of triglyceride (TG). Adipose tissue is also a major cholesterol storage organ. In obese humans, 33-50% of body cholesterol is found in adipose tissue, whereas it is about 25% in lean humans [1]. The majority of the adipocyte cholesterol is distribited in lipid droplets (LDs) in the forms of free cholesterol (FC) and cholesterol ester (CE) [2]. Indeed, cholesterol content in adipose tissue is generally proportional to the level of TG [1, 3]. Cholesterol uptake and intracellular cholesterol redistribution are closely associated with adipogenesis [4] and adipocyte expansion [5]. Moreover, suppressing cholesterol efflux in adipocytes leads to an increased intracellular cholesterol level with reduced LD size and TG content in adipocytes in obese mice [6], implicating a potential role of cholesterol in the development of adipose tissue and LDs. However, the key regulators of cholesterol homeostasis in adipocytes and related underlying mechanisms are poorly understood.

Cholesterol homeostasis is coordinately regulated by the uptake, synthesis, efflux and esterification of cholesterol [7]. Among these regulators, endoplasmic reticulum resident acyl-coenzyme A: cholesterol acyltransferases (ACATs, also known as sterol O-acyltransferases) catalyze the esterification of FC and long-chain fatty acid, mainly oleic and palmitic acids, to CE in the presence of ATP and coenzyme A [8]. ACAT has two

isoforms, ACAT1 [9], which is ubiquitously expressed in various tissues in mammals [10], and ACAT2 [11], which is mostly expressed in the intestine and liver [12]. Tissue distributions of ACAT1 and ACAT2 are similar across humans, mice, and monkeys, except in the liver, where humans express both ACAT1 and ACAT2 while mice and monkeys express mainly ACAT2 [10, 13, 14]. Since ACATs are the key enzymes for the control of CE synthesis and the availability of FC in cells, ACATs have been identified to be therapeutic targets for atherosclerosis [12], Alzheimer's disease [15] and several types of cancer [16-18].

Avasimibe (CI-1011) is a synthetic ACAT inhibitor [19] and has been developed for the treatment of atherosclerosis [20, 21]. Unlike other ACAT inhibitors, avasimibe displayed a human safety record with a minimal effect on adrenal toxicity [22]. Oral administration of avasimibe at a dosage range of 0.1-30 mg/kg/day is demonstrated to reduce the plasma total TG, very low-density lipoprotein (VLDL)-CE and VLDL-TG levels by 31%-48% in high-cholesterol or normal chow-fed animals [23-25]. In human clinic trials, oral administration of avasimibe at a dosage range of 50-500 mg/day lowered plasma TG and VLDL-cholesterol levels by 16-30% in patients with combined hyperlipidemia [26] without clinically meaningful changes in steroid hormone levels [27]. Compared with oral administration, non-oral administration appears to improve avasimibe blood bioavailability in non-hepatic tissues with no effect on cytotoxicity, body weight or adrenal gland [28]. Indeed, non-oral administration avasimibe helped us reveal a new role of ACAT in various

diseases, including prostate cancer [29], pancreatic ductal adenocarcinoma [30], hepatocellular carcinoma [31], chronic myelogenous leukemia [32], melanoma cancer immunotherapy [16], and Alzheimer's disease [33, 34].

Previously, we and others reported a positive correlation between *ACAT1* mRNA expression and adipogenesis *in vitro* as well as adiposity *in vivo* [35, 36]. We further showed that avasimibe suppressed LD formation and expansion during adipogenesis in 3T3-L1 cells [35]. Accordingly, we hypothesize that avasimibe attenuates the development of obesity.

To test this hypothesis, we investigated the role of non-orally administrated avasimibe in obesity using DIO mice. We found that avasimibe treatment promoted weight loss, particularly fat loss, with improved insulin sensitivity. The underlying mechanism involved suppressing food intake and reducing lipogenesis in adipose tissue. These results support the potential of using avasimibe to trigger weight loss via suppressing energy intake.

## 2. Materials and methods

### *2.1.Materials and reagents*

Free glycerol reagent (cat. no. F6428), glycerol standard solution (cat. no. G7793) and TG reagent (cat. no. T2449) were purchased from Sigma-Aldrich (St Louis, MO). TRIzol® reagent, SuperScriptII and Lipofectamine 2000 were from Invitrogen (Carlsbad, CA). Avasimibe (> 98% of purity) was from 2A Pharmachem (Lisle, IL), AdooQ bioscience

(Irvine, CA) or MedChemExpress (Shanghai, China). Protein assay kit and iTaq™ Universal SYBR® Green Supermix (cat. no. 172-5121) were from Bio-Rad Laboratories (Hercules, CA). Insulin ELISA kit (cat. no. 80-INSMSU-E01) was from Alpco Diagnostics (Salem, NH). Free fatty acid assay kit (cat. no. 700310) was brought from Cayman Chemical (Ann Arbor, MI). Cholesterol assay kit (cat. no. K603-100) was from BioVision (Milpitas, CA).

*2.2.Animal husbandry and administration of avasimibe*

Six to eight-week-old male C57BL/6J mice (The Jackson Laboratory, Bar harbor, ME) were fed with high-fat (HF) diet (60% of calories from fat, 0.035% cholesterol) (cat. no. TD.06414, Harlan Laboratories, Madison, WI, or cat. no. D12492i, Changzhou Shuyishuer Biotech, China) for 15 - 20 weeks to develop diet-induced obesity. These diet-induced obese (DIO) mice were then randomly assigned to control (CTRL) and avasimibe (AVA) groups. Avasimibe was dissolved in a vehicle solution (avasimibe first dissolved in dimethyl sulfoxide (DMSO) at a concentration of 90mg/ml, then diluted with 2-hydroxypropyl-β-cyclodextrin and Tween-80 in PBS, making the final concentration of avasimibe at 2.7mg/ml, DMSO at 3% (v/v), tween-80 at 2% (v/v) and 2-hydroxypropyl-β-cyclodextrin at 3.2mg/ml. We injected avasimibe solution or vehicle at 7.7ul /g body weight, corresponding to 20 mg/kg body weight, to the mice in the AVA and CTRL groups intraperitoneally (*i.p.*) daily for indicated days. The mice were kept on a 12/12 h light/dark

cycle at 22 - 25°C, with HF diet and water *ad libitum*. Food and body weight were determined every other day or daily. Experimental procedures were approved by the Purdue University Institutional Animal Care and Use Committee (protocol no. 1112000347) and Hong Kong Polytechnic University Animal Subjects Ethics Sub-committee.

*2.3.Pair-feeding study*

DIO C57BL/6J mice (male, 29-37 weeks of age) were randomly assigned to CTRL, AVA and pair-feeding (Pair) groups. Mice from the AVA group received a 20 mg/kg body weight dosage of avasimibe through daily *i.p.* injection, while mice from the CTRL and PAIR groups received vehicle solution. The food intake of these mice was measured twice daily, at the beginning of the light and dark cycles. Thus, the food consumption during the light cycle was calculated by (food amount in the cage at 7 am – food amount in the cage at 7 pm). Food consumption during the dark cycle was calculated by (food amount in the cage at 7 pm – food amount in the cage at 7 am the next day). The restricted-food administration of Pair group was staggered one day later than the treatment of CTRL and AVA groups. All the Pair mice were given the same amount of food consumed by the AVA mice on the previous day. The mice in the CTRL and AVA groups were allowed to access the HF diet *ad libitum*. All the mice used in this study were allowed to access water *ad*

*libitum.* Body weight was monitored every day. Experimental procedures were approved by the Purdue University Institutional Animal Care and Use Committee.

*2.4.Metabolic chamber measurement*

An indirect Calorimeter (Oxymax, Columbus Instruments, model: Open Circuit Indirect Calorimeter) was employed to measure oxygen ($O_2$) consumption and carbon dioxide ($CO_2$) production. Mice were housed individually with a 12/12 h light/dark cycle at 26°C for indicated days with *ad libitum* access to diet and water (mice in Pair group were given a defined amount of food as described above) for four days. The metabolic chamber detected $VO_2$ and $VCO_2$ every 22 minutes. Data of two dark cycles (7 pm-7 am) and two light cycles (7 am-7 pm), *i.e*. data collected from the 21$^{st}$ hr to 69$^{th}$ hr in the metabolic chambers, were used to calculate the respiratory exchange ratio [37] and energy expenditure by [3.815 x $VO_2$ (L/h) + 1.232 x $VCO_2$ (L/h)]/lean mass (kg).

*2.5.Fecal calorie measurement and Dual-energy X-ray absorptiometry (DEXA) analysis*

Fecal samples were collected from the individual cage for further analysis as described previously [38, 39]. At the end of the study, mice were euthanized with $CO_2$, and scanned for body composition by a PIXImus densitometer (Lunar; GE-Healthcare, Madison, WI) as described previously [40].

*2.6.Blood collection, hormone and metabolite measurements from mouse serum*

For 6 hr fasting blood glucose level determination, we fasted mice during the light cycle, *i.e.* we removed food at 9:30 am and measured blood glucose level at 3:30 pm. At the end of the study, blood samples were collected from overnight fasted mice through cardio-puncture. After clotting at room temperature for ~15min, blood samples were centrifuged at 2,000g for 10 min to get the supernatants. Serum levels of insulin and leptin were determined by the corresponding ELISA kits, and the serum levels of alanine transaminase (ALT), cholesterol, glycerol and free fatty acids were determined by appropriate kits as described in materials and reagents. All assays were performed according to the manufacturer's instructions.

*2.7.Intraperitoneal glucose tolerance test (IPGTT) and homeostatic model assessment of insulin resistance (HOMA-IR)*

IPGTT was performed following the standard protocol. After fasting mice for 12 h, blood was taken from their tails to measure the basal glucose level. Glucose concentration was determined using a glucometer (Bayer Healthcare LLC, Mishawka, IN). Mice were injected intraperitoneally with 50 % glucose solution at 1.5 g/kg body weight. After injection, blood was drawn from the tail vein at 0, 15, 30, 45, 60, and 120 min for the determination of blood glucose concentration. Serum insulin and glucose level from the overnight fasted mice were determined as described above, and HOMA-IR was calculated

based on the following equation: HOMA-IR = fasting plasma insulin (mU/L) × fasting plasma glucose (mg/dl)/405 [41, 42].

*2.8.Quantitative real-time PCR*

The total RNA was isolated from adipose tissue using TriZol reagent (Invitrogen, Carlsbad, CA, USA) and subsequently, isolated RNA was reverse transcribed to cDNA by the SuperScript II kit (Invitrogen) according to the manufacturer's protocol. mRNA level of each gene was quantified by real-time PCR using iTaq™ Universal SYBR® Green Supermix (Applied Biosystems, Carlsbad, CA) containing 100 ng/ml PCR primers by StepOne Real-Time PCR System (Applied Biosystems, Carlsbad, CA). Table S1 shows the sequence of primer sets used in this study. The mRNA levels were normalized to ribosomal protein L27 (*RPL27)* (an 18S ribosomal protein) or β-actin and calculated with the comparative CT method. Data were normalized to *RPL27* or β-actin as indicated and analyzed by △△Ct method.

*2.9.Statistical Analysis*

Data are presented as means ± SEM. Statistical analysis was performed using Student's two-tailed t-test to compare between groups. One-way ANOVA with Bonferroni post hoc test was performed to analyze the data in Fig. 5 D and H with SAS 9.2 (SAS® Inst. Inc., Cary, NC). A *P*-value of less than 0.05 was considered statistically significant.

## 3. **Results**

### *3.1.Non-oral administration of avasimibe reduces body weight via suppressing food intake in high-fat diet-induced obese mice*

Among several animal models of obesity [43], we chose the DIO mouse model since it mimics obesity development in humans better than other models. We fed six- to eight-week-old male mice (C57BL/6J) with HF diet (60 % calorie from fat) *ad libitum* for fifteen to twenty weeks to develop obesity. These DIO mice (49.96 ± 1.21 g) were randomly assigned into two groups to receive vehicle (CTRL) or *i.p.* injection of avasimibe (AVA, 20 mg/kg body weight) daily for thirteen days. The dosage of avasimibe was determined based on previous studies [22, 29]. At the end of the study, we sacrificed mice after overnight fasting and collected various samples for further analyses. We assessed the cytotoxicity by measuring serum ALT activity and found that avasimibe administration showed little effect on the serum ALT level (33.79 ± 18.35 IU/L vs. 29.56 ± 9.74 IU/L) (Fig. 1A). Administration of avasimibe significantly reduced the body weight of DIO mice compared to the mice in the CTRL group (49.91 ± 1.09 g vs. 38.47 ± 1.06 g) at the end of the study (Fig. 1B), corresponding to 22.2 ± 1.8 % weight loss relative to their initial weights (Fig. 1C). Consistent with these results, obese mice receiving low dose avasimibe (10 mg/kg body weight via *i.p.* administration) resulted in approximately 24 % decrease in body weight(Fig. S1A). Mice in the AVA group displayed a 38% less fat mass than the CTRL group with a 42 % body fat content as compared to 49 % in the CTRL group (Fig.

1D). Interestingly, mice in the AVA group showed a 3.38g less lean mass than mice in the CTRL group with a 57 % lean body content as compared to 51 % in the CTRL group (Fig. 1D). While there was a significant decrease in inguinal, epididymal and retroperitoneal fat pad weight (Fig. 1E) in the AVA mice, no significant differences in liver and heart weight (Fig. 1F), and bone density (Fig. S2) were observed between the two groups. Evidently, kidney weight was lower in mice in the AVA group than those in the CTRL group (0.37 ± 0.01 g vs. 0.42 ± 0.01 g). Thus, the weight loss induced avasimibe treatment was mainly attributed to the loss of fat mass in DIO mice.

We next sought to determine whether the avasimibe-reduced fat mass was attributed to the reduction of energy intake or energy expenditure. We, thus, quantified the effects of avasimibe on food intake and metabolic activity of DIO mice. While mice in the CTRL group consumed 2.49 ± 0.11 g food/day/mouse, mice in the AVA groups showed reduced food intake at 1.24 ± 0.15 g/day/mouse, resulting in a 50 % decrease in food intake (Fig. 2A). We observed that this reduction in food intake was steady throughout the 13-day experimental period. Consistent with this result, obese mice receiving low dose avasimibe (10 mg/kg body weight via *i.p.* administration) resulted in 63.6 % decrease in food intake (Fig. S1B). On the other hand, administration of avasimibe (20 mg/kg body weight) to lean mice fed with HF diet for 30 days resulted in a 15% decrease in daily food intake and a 14% decrease in body weight (Fig. S3).

Next, we examined the effect of avasimibe administration on the energy expenditure in these mice using a metabolic chamber. Compared with the mice in the CTRL group, mice in the AVA group had higher energy expenditure both in dark and light cycles (Fig. 2B and D), indicating a potential role of avasimibe in increasing basal metabolism. Moreover, avasimibe-treated mice had a lower respiratory exchange ratio (RER) than vehicle-treated mice both in dark and light cycles (Figs. 2C and E), indicating a shift in substrate utilization towards enhanced lipid oxidation in the avasimibe-treated mice. Collectively, our results indicate that an acute *i.p.* administration of avasimibe ameliorates obesity in DIO mice through reducing body fat mass, food intake, and increasing lipid usage in energy balance.

### *3.2.Non-oral administration of avasimibe ameliorates systemic glucose homeostasis in DIO mice*

Since obesity enhances the risks of insulin resistance and glucose intolerance, we next examined whether avasimibe could improve glucose homeostasis in DIO mice. Even after three days of avasimibe treatment, mice in the AVA group had a lower blood glucose level after fasting for 6 h (157.5 ± 10.6 mg/dL) compared with the mice in the CTRL group (194.7 ± 12.9 mg/dL) (Fig. 3A) even though mice in the two groups showed no significant differences in body weight. After 11 days of avasimibe treatment, we performed an IPGTT. Avasimibe-treated mice exhibited a faster clearance rate of circulating glucose than those

in the CTRL group (Fig. 3B), as indicated by a 49.3% reduction of the area under the curve (Fig. 3C). Mice in the AVA group also showed a marked decrease in serum insulin level (0.31 ± 0.05 ng/ml) and HOMA-IR index (1.77 ± 0.34) after overnight fasting, compared with those of mice in the CTRL group (2.44 ± 0.31ng/mL and 26.67 ± 4.57) (Figs. 3D and E). Moreover, avasimibe treatment resulted in a decrease in serum FC (0.35 ± 0.07 mM) (Fig. 3F), CE (1.03 ± 0.26 mM) (Fig. 3G) and TG (0.60 ± 0.07 mM (Fig. 3H) compared with those in the CTRL group (FC: 1.41 ± 0.42 mM; CE: 7.52 ± 0.96 mM; TG: 1.41 ± 0.13 mM). However, avasimibe treatment showed no effect on the serum glycerol and free fatty acids levels (Figs. 3I and J). These results indicate that *i.p.* administration of avasimibe improves glucose homeostasis and serum lipid profiles in DIO mice.

### *3.3.Non-oral administration of avasimibe lowers the expression of adipocyte-specific genes in white adipose tissue of DIO mice*

We previously reported that avasimibe suppressed *de novo* lipogenesis in adipocytes *in vitro* by down-regulating the expression of the genes involved in lipid synthesis [35]. Here, we tested whether avasimibe administration could exhibit a similar effect *in vivo*. We found that epididymal white adipose tissue (epiWAT) from the mice in the AVA group showed a marked reduction of the mRNA levels of adipogenic genes such as *PPAR* and *SREBP1c*, and their downstream genes such as *FAS* and *SCD1* compared with those in the CTRL group (Fig. 4A). Avasimibe-treated mice exhibited substantially decreased mRNA levels

of the genes involved in TG synthesis, such as *MGAT1* and *DGAT2*. However, there is no difference in the mRNA levels of genes involved in cholesterol homeostasis in epiWAT, including *SREBP1*, *SREBP2*, and *LDLR* (Fig. 4A). Consistent with the avasimibe-induced decrease in adipose tissue weight shown in Fig. 1E, avasimibe-treated DIO mice also displayed a reduction of *Leptin* and *Adiponectin* mRNA levels in epiWAT (Fig. 4B), as well as serum leptin level (Fig. 4C). Obesity is associated with adipose tissue pathology, including macrophage infiltration, low-grade inflammation, macrophage switch from alternatively activated M2 to pro-inflammatory M1 type, and fibrosis [44-47]. We next investigated the effect of avasimibe administration on the mRNA levels of inflammatory cytokines (*MCP1*, *IL-6*, *TNFα*, *CCL5*, and *CCL7*), pan-macrophage marker genes (*CD68* and *F4/80*), M2 macrophage marker genes (*MGL2* and *ARG1*), and fibrosis (*TGFb1* and *MMP2*) in adipose tissue isolated from the CTRL and AVA groups. Mice in both groups showed similar mRNA levels of inflammatory genes, such as *MCP1*, *IL-6*, *TNFα*, *CCL5*, and *CCL7* (Fig. 4D and E). As shown in Fig. 4E, a 13-day avasimibe administration exerted no effect on the mRNA levels of *CD68*, *F4/80*, *MGL2*, *CCL5*, *CCL7*, *TGFb1*, and *MMP2*. Interestingly, avasimibe administration resulted in a marked increase (an 8.7-fold) in *ARG1* level in adipose tissue.

We also found that avasimibe treatment resulted in increased hepatic TG level and a decrease in *SCD1* expression in the liver. However, avasimibe treatment showed no effect on the hepatic total cholesterol level and the mRNA levels of the genes in *de novo*

lipogenesis (*SREBP1c* and *FAS*) and cholesterol synthesis and metabolism (*SREBP2*, *HMGCR*, *HMGCS2* and *NR1H3*/*LXR*$\alpha$) in the liver (Fig. S4). Collectively, *i.p.* administration of avasimibe inhibited mRNA levels of genes involved in *de novo* lipogenesis and adiposity with little effect on improving adipose pathology in epiWAT of DIO mice.

### *3.4.Avasimibe-induced body weight loss in DIO mice is largely attributed to the suppression of food intake*

The difference in food intake between the two groups prompted us to hypothesize that avasimibe-induced weight loss in DIO mice was resulted from suppression of obesity-associated food intake. To test this, we first examined the effect of *i.p.* administration of avasimibe on the expression of the genes involved in appetite control and inflammation in the hypothalamus. We found that the hypothalamus isolated from the mice in the AVA group exhibited a marked reduction of the mRNA levels of orexigenic genes (*NPY* and *AGRP*) and *CART* with no effect on other anorexigenic genes (*POMC* and *MC4R*) compared with those in the CTRL group (Fig. 5A). Moreover, avasimibe treatment markedly suppressed mRNA levels of *TNF*$\alpha$ and *IL1*$\beta$ in the hypothalamus (Fig. 5A). To further investigate the anti-obesity mechanism of avasimibe, we conducted a pair-feeding experiment, in which DIO mice were randomly assigned to one of the following three groups: vehicle-treated (CTRL), avasimibe-treated (AVA) and pair-fed (Pair) groups. Pair-

fed mice were fed the same amount of HF diet as the mice in the AVA group had consumed in the previous day. Mice in both the CTRL and AVA groups were given HF diet *ad libitum*. As shown in Fig. 5, DIO mice from both the AVA and Pair groups had similar reductions in body weight during an 8-day experiment compared with those in the CTRL group (Figs. 5B and C), indicating the weight loss in the avasimibe-treated mice was, at least in part, resulted from reduced food intake mostly in the dark cycle (Fig. 5D). Interestingly, avasimibe-treated mice showed a 2.6 % decrease in RER values than the mice in the PAIR group in the dark cycle (0.76 ± 0.003 vs. 0.78 ± 0.003) (Fig. 5E). Moreover, in the light cycle avasimibe-treated mice had higher energy expenditure than those in the Pair group (Fig. 5F). Next, we examined the effect of avasimibe treatment on the amount of energy in the food that was lost in the excreta examined by fecal excretion and fecal energy density. Both the AVA and Pair groups showed significantly lower daily fecal excretion compared with the CTRL group (Fig. 5G). Evidently, the feces excreted from avasimibe-treated mice contained a slightly higher level of energy density than those in the CTRL or Pair groups (Fig. 5H, 4.60 ± 0.06 vs. 4.34 ± 0.05 or 4.35 ± 0.06 kcal/g). These results indicate that the body weight loss induced by avasimibe treatment was largely attributed to avasimibe-suppressed food intake.

## 4. **Discussion**

Although the role of ACAT in cholesterol metabolism and atherosclerosis is well documented, its role in adiposity and the development of obesity remains elusive. Previously, we reported that ACAT is required for lipogenesis in adipocytes *in vitro* and highlighted the important role of ACAT in integrating cholesterol metabolism and TG synthesis in adipocytes [35]. This notion was further supported by a recent study in which ACAT overexpression resulted in increased free cholesterol on the LD surface with impeding adipocyte function [36]. These led us to hypothesize that ACAT serves as a therapeutic target for the treatment of adiposity and its related metabolic disorders. Herein, we showed for the first time that non-oral *i.p.* administration of avasimibe decreased body weight and fat mass with improved insulin sensitivity and serum lipid profile and suppressed adipocyte lipogenesis in epididymal fat in DIO mice. However, avasimibe administration exerted little effect on improving adipose pathology and lipid metabolism in the liver in DIO mice. Intriguingly, we observed a marked suppression of food intake in avasimibe-treated DIO mice with an increase in energy expenditure, basal metabolism, and a shift in fuel preference towards lipids, indicating a potential function of avasimibe in lowering obesity-related hyperphagia. In support of this view, our pair-feeding study further revealed that avasimibe's anti-obesity effect was predominantly attributed to suppressed food intake. Moreover, avasimibe administration presented a higher basal metabolic rate than the pair-feeding regime. Based on these results, we speculate an anti-obesity potential of avasimibe. It should be noted that avasimibe's ability to lower body

weight and food intake appears to be maximized when it is administrated to obese animals since *i.p.,* injection of avasimibe (20mg/kg body weight) to lean mice for 30 days did not show a dramatic decrease in food intake or weight loss (Fig. S3). In support, *i.p.* administration of avasimibe into cancer-bearing non-obese mice for 25-day [48] and 4-week [49] resulted in no cytotoxicity with no changes in body weight and food intake.

Evidently, our finding of avsimibe's anti-obesity effect is likely to depend on the drug administration route since such a result was shown when avasimibe was administrated intraperitoneally in DIO mice but not by oral administration (data not shown). Similarly, orally administrated avasimibe showed no effects on the body weight or food intake in human atherosclerotic lesions [21] and various animal models of diseases such as atherosclerosis [50] and hypercholesterolemia [51]. Comparing to oral administration, non-orally administrated avasimibe was shown to improve blood bioavailability and its concentration in non-hepatic tissues [28]. In support, non-oral administration of avasimibe has been shown to successfully target ACAT-regulated cholesterol metabolism in various tissues for the treatment of Alzheimer's disease, chemo-immunotherapy, lung cancer, prostate cancer, pancreatic cancer, and hepatocellular carcinoma [16, 28-30, 33, 48, 52].

It should be noted that *ACAT1* or *ACAT2* knockout mice exhibited little or no change in body weight and food intake when fed with a standard or high cholesterol diet [20]. However, in agreement with our findings, Xu et al. demonstrated that diet-induced obesity and insulin resistance were significantly attenuated in *ACAT1* knockout mice when

challenged with a HF diet [53]. Moreover, HF diet-altered food intake-regulating signaling and inflammation in the hypothalamus were reported to be alleviated in *ACAT1* knockout mice, which in turn contributed to the protecting the mice from HF diet-induced insulin resistance and cognitive impairment in the hippocampus. Collectively, these results and our present study underscore the important role of ACAT-regulated brain cholesterol metabolism in HF diet-induced obesity.

Besides its structural role in the plasma membrane and myelin production [54], brain cholesterol metabolism plays a critical role in the function of the central nervous system (CNS), and the systemic energy metabolism as reduced *de novo* cholesterol synthesis and/or accumulation of CE in the brain is associated with, in part, Alzheimer's disease [55], Huntington's disease, Parkinson's disease [56], diabetes and its related food intake [57], Niemann-Pick disease type C and Smith-Lemli-Opitz syndrome [58]. Additionally, plasma membrane cholesterol in the hypothalamus is reported to be required for constitutive endocytosis of melanocortin-4 receptor (MC4R), a central regulator of food intake, and its responsiveness to MC4R agonist melanocyte-stimulating hormone (MSH) for proper control of appetite [59]. Moreover, HF diet feeding is associated with reduced cholesterol synthesis [57], elevated levels of ACAT1 [60] in the hypothalamus, and an increase in CE in the aged brain [61]. These studies imply a beneficial role of maintaining a brain unesterified cholesterol pool for the promotion of CNS functions and energy metabolism. In support, *ACAT1* ablation [62] and non-oral administration of ACAT inhibitors, such as

avasimibe [33], CP-113,818 [63], and K-604 [64], have been reported to elevate the levels of unesterified cholesterol and 24-hydroxycholestgerol with suppression of CE level, ACAT activity and/or amyloid- βexpression in the brains of mouse models of Alzheimer's disease. These studies further imply a therapeutic potential of some of the ACAT inhibitors for the diseases related to ACAT-dysregulated brain cholesterol metabolism and energy balance through penetrating the blood-brain barrier. In support of this notion, our *i.p.* injection of avasimibe to DIO mice decreased the levels of the genes involved in appetite control and inflammation in the hypothalamus (Fig. 5A).

Our study has some limitations that may lead to future avenues of research. While our study aimed to elucidate the therapeutic potential of avasimibe in obesity, future study should focus on elucidating the mechanism underlying the inhibitory effect of avasimibe on food intake and obesity using DIO and/or tissue-specific *ACAT1* knockout mice. As global *ACAT1* knockout protected mice from HF diet-induced hypothalamic inflammation, insulin resistance and neuropeptide dysregulation [53], evaluation of the direct role of avasimibe and brain-specific deficiency of *ACAT1* in central regulation of obesity-related metabolic and eating disorders warrants future studies. Although out study employed prolonged HF diet-induced obesity model, other genetic models of obesity could be used to recapitulate the anti-obesity function of avasimibe and ACAT inhibitors. Our study largely relies on fixed avasimibe doses (*i.e.*, 10 mg/kg and 20 mg/kg) to test its anti-obesity effect. This should be followed by investigation of dose-dependent effect of avasimibe and

ACAT inhibitors on obesity to determine the lowest effective dose of ACAT inhibitors for lowering body weight and food intake in obese animals. Herein, we demonstrated a non-cytotoxic effect of non-orally administrated avasimibe in obese mice by measuring ALT activity. However, this does not rule out the possibility of avasimibe-related locomotor and behavioral dysfunction. Indeed, our preliminary assessment of the effect of avasimibe on locomotor activity in obese mice showed that avasimibe-treatment resulted in lower total distance, total distance in side, total distance in arena, and cumulative duration in center with slight increase in cumulative duration in side and no change in rearing duration (Fig. S5). These results bring the possibility of a potential effect of avasimibe-regulated food intake and energy balance on the changes in locomotor activity and behavior, which underscores the need to understand the mechanisms by which avasimibe influences locomotor behavior.

In conclusion, we demonstrate that avasimibe, a clinically safe and efficacious ACAT inhibitor, can potentially treat obesity and insulin resistance through suppression of food intake. Our findings indicate that avasimibe could be an efficient therapy in the pharmacological treatment of obesity with hyperphagia.

## Author contributions

Zhu, Y. designed and analyzed the research, performed all the experiments, and wrote the manuscript. Kim, K.-H. designed, analyzed, and supervised the research and wrote the manuscript. Kim, S.Q., Zhang Y. and Liu, Q. analyzed data and prepared the manuscript. The manuscript was critically reviewed and approved by all authors.


## Acknowledgments

We thank Kimberly K. Buhman, Scott A. Crist and Lihao Huang for their insightful comments; Kolapo Ajuwon, Jonathan C Kershaw, Jordan Oshiro, Siyuan Sheng and Zhihong Song, Patricia Jaynes and Sydney E. Moser for their technical assistance. We thank Benjamin Yee for assistance in behavior experiment design. We also acknowledge Ko Chi-bun Ben and Pan Xiaohan for their assistance with the use of a high-content imaging system supported by Collaborative Research Fund, Hong Kong Research Grants Council #C5012-15E, and animal experiment.

## Funding:

This work was supported, in part, by Purdue Research Foundation, Ralph W. and Grace M. Showalter Research Trust, the USDA National Institute of Food and Agriculture Hatch project (No. 1013613) for K.-H.K., and by the Hong Kong Polytechnic University (No:

P0030234 and No: P0036229) and the Hong Kong Research Grants Council (No. 25100420) for Y.Z.

**Conflict of interest**

K.-H.K. is a founder and shareholder of EFIL Bioscience Incorporation. The other author declares no conflict of interest. K.-H.K. and Y.Z. are inventors on a patent filed by Purdue University covering the compositions and methods for regulating body weight and metabolic syndromes.

## REFERENCES


[1] Schreibman PH, Dell RB. Human adipocyte cholesterol. Concentration, localization, synthesis, and turnover. J Clin Invest. 1975;55:986-93.

[2] Krause BR, Hartman AD. Adipose tissue and cholesterol metabolism. J Lipid Res. 1984;25:97-110.

[3] Kovanen PT, Nikkila EA, Miettinen TA. Regulation of cholesterol synthesis and storage in fat cells. J Lipid Res. 1975;16:211-23.

[4] Dagher G, Donne N, Klein C, Ferre P, Dugail I. HDL-mediated cholesterol uptake and targeting to lipid droplets in adipocytes. J Lipid Res. 2003;44:1811-20.

[5] Le Lay S, Krief S, Farnier C, Lefrere I, Le Liepvre X, Bazin R, et al. Cholesterol, a cell size-dependent signal that regulates glucose metabolism and gene expression in adipocytes. J Biol Chem. 2001;276:16904-10.

[6] Cuffe H, Liu M, Key CC, Boudyguina E, Sawyer JK, Weckerle A, et al. Targeted Deletion of Adipocyte Abca1 (ATP-Binding Cassette Transporter A1) Impairs Diet-Induced Obesity. Arterioscler Thromb Vasc Biol. 2018;38:733-43.

[7] Luo J, Yang H, Song BL. Mechanisms and regulation of cholesterol homeostasis. Nat Rev Mol Cell Biol. 2020;21:225-45.

[8] Mukherjee S, Kunitake G, Alfin-Slater RB. The esterification of cholesterol with palmitic acid by rat liver homogenates Journal of Biological Chemistry. 1958;230:91-6.

[9] Chang CC, Huh HY, Cadigan KM, Chang TY. Molecular cloning and functional expression of human acyl-coenzyme A:cholesterol acyltransferase cDNA in mutant Chinese hamster ovary cells. J Biol Chem. 1993;268:20747-55.

[10] Meiner V, Tam C, Gunn MD, Dong LM, Weisgraber KH, Novak S, et al. Tissue expression studies on the mouse acyl-CoA: cholesterol acyltransferase gene (Acact): findings supporting the existence of multiple cholesterol esterification enzymes in mice. J Lipid Res. 1997;38:1928-33.

[11] Cases S, Novak S, Zheng YW, Myers HM, Lear SR, Sande E, et al. ACAT-2, a second mammalian acyl-CoA:cholesterol acyltransferase. Its cloning, expression, and characterization. J Biol Chem. 1998;273:26755-64.

[12] Chang TY, Li BL, Chang CC, Urano Y. Acyl-coenzyme A:cholesterol acyltransferases. Am J Physiol Endocrinol Metab. 2009;297:E1-9.

[13] Lee RG, Willingham MC, Davis MA, Skinner KA, Rudel LL. Differential expression of ACAT1 and ACAT2 among cells within liver, intestine, kidney, and adrenal of nonhuman primates. J Lipid Res. 2000;41:1991-2001.

[14] Parini P, Davis M, Lada AT, Erickson SK, Wright TL, Gustafsson U, et al. ACAT2 is localized to hepatocytes and is the major cholesterol-esterifying enzyme in human liver. Circulation. 2004;110:2017-23.

[15] Shibuya Y, Chang CC, Chang TY. ACAT1/SOAT1 as a therapeutic target for Alzheimer's disease. Future Med Chem. 2015;7:2451-67.
[16] Yang W, Bai Y, Xiong Y, Zhang J, Chen S, Zheng X, et al. Potentiating the antitumour response of CD8(+) T cells by modulating cholesterol metabolism. Nature. 2016;531:651-5.
[17] Zabielska J, Sledzinski T, Stelmanska E. Acyl-Coenzyme A: Cholesterol Acyltransferase Inhibition in Cancer Treatment. Anticancer Res. 2019;39:3385-94.
[18] Song BL, Wang CH, Yao XM, Yang L, Zhang WJ, Wang ZZ, et al. Human acyl-CoA:cholesterol acyltransferase 2 gene expression in intestinal Caco-2 cells and in hepatocellular carcinoma. The Biochemical journal. 2006;394:617-26.
[19] Burnett JR, Huff MW. Avasimibe Pfizer. Curr Opin Investig Drugs. 2002;3:1328-33.
[20] Llaverias G, Laguna JC, Alegret M. Pharmacology of the ACAT inhibitor avasimibe (CI-1011). Cardiovasc Drug Rev. 2003;21:33-50.
[21] Tardif JC, Gregoire J, L'Allier PL, Anderson TJ, Bertrand O, Reeves F, et al. Effects of the acyl coenzyme A:cholesterol acyltransferase inhibitor avasimibe on human atherosclerotic lesions. Circulation. 2004;110:3372-7.
[22] Robertson DG, Breider MA, Milad MA. Preclinical safety evaluation of avasimibe in beagle dogs: an ACAT inhibitor with minimal adrenal effects. Toxicol Sci. 2001;59:324-34.
[23] Lee HT, Sliskovic DR, Picard JA, Roth BD, Wierenga W, Hicks JL, et al. Inhibitors of acyl-CoA: cholesterol O-acyl transferase (ACAT) as hypocholesterolemic agents. CI-1011: an acyl sulfamate with unique cholesterol-lowering activity in animals fed noncholesterol-supplemented diets. J Med Chem. 1996;39:5031-4.
[24] Ramharack R, Spahr MA, Sekerke CS, Stanfield RL, Bousley RF, Lee HT, et al. CI-1011 lowers lipoprotein(a) and plasma cholesterol concentrations in chow-fed cynomolgus monkeys. Atherosclerosis. 1998;136:79-87.
[25] Burnett JR, Wilcox LJ, Telford DE, Kleinstiver SJ, Barrett PH, Newton RS, et al. Inhibition of ACAT by avasimibe decreases both VLDL and LDL apolipoprotein B production in miniature pigs. J Lipid Res. 1999;40:1317-27.
[26] Insull W, Jr., Koren M, Davignon J, Sprecher D, Schrott H, Keilson LM, et al. Efficacy and short-term safety of a new ACAT inhibitor, avasimibe, on lipids, lipoproteins, and apolipoproteins, in patients with combined hyperlipidemia. Atherosclerosis. 2001;157:137-44.
[27] Raal FJ, Marais AD, Klepack E, Lovalvo J, McLain R, Heinonen T. Avasimibe, an ACAT inhibitor, enhances the lipid lowering effect of atorvastatin in subjects with homozygous familial hypercholesterolemia. Atherosclerosis. 2003;171:273-9.
[28] Lee SS, Li J, Tai JN, Ratliff TL, Park K, Cheng JX. Avasimibe encapsulated in human serum albumin blocks cholesterol esterification for selective cancer treatment. ACS Nano. 2015;9:2420-32.

[29] Yue S, Li J, Lee SY, Lee HJ, Shao T, Song B, et al. Cholesteryl ester accumulation induced by PTEN loss and PI3K/AKT activation underlies human prostate cancer aggressiveness. Cell Metab. 2014;19:393-406.
[30] Li J, Qu X, Tian J, Zhang JT, Cheng JX. Cholesterol esterification inhibition and gemcitabine synergistically suppress pancreatic ductal adenocarcinoma proliferation. PLoS One. 2018;13:e0193318.
[31] Jiang Y, Sun A, Zhao Y, Ying W, Sun H, Yang X, et al. Proteomics identifies new therapeutic targets of early-stage hepatocellular carcinoma. Nature. 2019;567:257-61.
[32] Bandyopadhyay S, Li J, Traer E, Tyner JW, Zhou A, Oh ST, et al. Cholesterol esterification inhibition and imatinib treatment synergistically inhibit growth of BCR-ABL mutation-independent resistant chronic myelogenous leukemia. PLoS One. 2017;12:e0179558.
[33] Huttunen HJ, Havas D, Peach C, Barren C, Duller S, Xia W, et al. The acyl-coenzyme A: cholesterol acyltransferase inhibitor CI-1011 reverses diffuse brain amyloid pathology in aged amyloid precursor protein transgenic mice. J Neuropathol Exp Neurol. 2010;69:777-88.
[34] Huttunen HJ, Peach C, Bhattacharyya R, Barren C, Pettingell W, Hutter-Paier B, et al. Inhibition of acyl-coenzyme A: cholesterol acyl transferase modulates amyloid precursor protein trafficking in the early secretory pathway. FASEB J. 2009;23:3819-28.
[35] Zhu Y, Chen CY, Li J, Cheng JX, Jang M, Kim KH. In vitro exploration of ACAT contributions to lipid droplet formation during adipogenesis. J Lipid Res. 2018;59:820-9.
[36] Xu Y, Du X, Turner N, Brown AJ, Yang H. Enhanced acyl-CoA:cholesterol acyltransferase activity increases cholesterol levels on the lipid droplet surface and impairs adipocyte function. J Biol Chem. 2019;294:19306-21.
[37] Henagan TM, Lenard NR, Gettys TW, Stewart LK. Dietary quercetin supplementation in mice increases skeletal muscle PGC1alpha expression, improves mitochondrial function and attenuates insulin resistance in a time-specific manner. PLoS One. 2014;9:e89365.
[38] Murphy EF, Cotter PD, Healy S, Marques TM, O'Sullivan O, Fouhy F, et al. Composition and energy harvesting capacity of the gut microbiota: relationship to diet, obesity and time in mouse models. Gut. 2010;59:1635-42.
[39] Kim CY, Zhu YY, Buhman KK, Kim KH. Dietary selenate attenuates adiposity and improves insulin sensitivity in high-fat diet-induced obese mice. J Funct Foods. 2015;17:33-42.
[40] Xue Y, Fleet JC. Intestinal vitamin D receptor is required for normal calcium and bone metabolism in mice. Gastroenterology. 2009;136:1317-27, e1-2.
[41] Matthews DR, Hosker JP, Rudenski AS, Naylor BA, Treacher DF, Turner RC. Homeostasis model assessment: insulin resistance and beta-cell function from fasting plasma glucose and insulin concentrations in man. Diabetologia. 1985;28:412-9.

[42] Wallace TM, Levy JC, Matthews DR. Use and abuse of HOMA modeling. Diabetes Care. 2004;27:1487-95.
[43] Kleinert M, Clemmensen C, Hofmann SM, Moore MC, Renner S, Woods SC, et al. Animal models of obesity and diabetes mellitus. Nat Rev Endocrinol. 2018;14:140-62.
[44] Datta R, Podolsky MJ, Atabai K. Fat fibrosis: friend or foe? JCI Insight. 2018;3.
[45] Huang LH, Melton EM, Li H, Sohn P, Jung D, Tsai CY, et al. Myeloid-specific Acat1 ablation attenuates inflammatory responses in macrophages, improves insulin sensitivity, and suppresses diet-induced obesity. Am J Physiol Endocrinol Metab. 2018;315:E340-E56.
[46] Lin, Chun TH, Kang L. Adipose extracellular matrix remodelling in obesity and insulin resistance. Biochem Pharmacol. 2016;119:8-16.
[47] Reilly SM, Saltiel AR. Adapting to obesity with adipose tissue inflammation. Nat Rev Endocrinol. 2017;13:633-43.
[48] Bi M, Qiao X, Zhang H, Wu H, Gao Z, Zhou H, et al. Effect of inhibiting ACAT-1 expression on the growth and metastasis of Lewis lung carcinoma. Oncol Lett. 2019;18:1548-56.
[49] Li J, Gu D, Lee SS, Song B, Bandyopadhyay S, Chen S, et al. Abrogating cholesterol esterification suppresses growth and metastasis of pancreatic cancer. Oncogene. 2016;35:6378-88.
[50] Delsing DJ, Offerman EH, van Duyvenvoorde W, van Der Boom H, de Wit EC, Gijbels MJ, et al. Acyl-CoA:cholesterol acyltransferase inhibitor avasimibe reduces atherosclerosis in addition to its cholesterol-lowering effect in ApoE*3-Leiden mice. Circulation. 2001;103:1778-86.
[51] Post SM, Zoeteweij JP, Bos MH, de Wit EC, Havinga R, Kuipers F, et al. Acyl-coenzyme A:cholesterol acyltransferase inhibitor, avasimibe, stimulates bile acid synthesis and cholesterol 7alpha-hydroxylase in cultured rat hepatocytes and in vivo in the rat. Hepatology. 1999;30:491-500.
[52] Pan J, Zhang Q, Palen K, Wang L, Qiao L, Johnson B, et al. Potentiation of Kras peptide cancer vaccine by avasimibe, a cholesterol modulator. EBioMedicine. 2019;49:72-81.
[53] Xu N, Meng H, Liu TY, Feng YL, Qi Y, Zhang DH, et al. Sterol O-acyltransferase 1 deficiency improves defective insulin signaling in the brains of mice fed a high-fat diet. Biochem Biophys Res Commun. 2018;499:105-11.
[54] Dietschy JM, Turley SD. Thematic review series: brain Lipids. Cholesterol metabolism in the central nervous system during early development and in the mature animal. J Lipid Res. 2004;45:1375-97.
[55] Puglielli L, Tanzi RE, Kovacs DM. Alzheimer's disease: the cholesterol connection. Nat Neurosci. 2003;6:345-51.

[56] Block RC, Dorsey ER, Beck CA, Brenna JT, Shoulson I. Altered cholesterol and fatty acid metabolism in Huntington disease. J Clin Lipidol. 2010;4:17-23.
[57] Suzuki R, Lee K, Jing E, Biddinger SB, McDonald JG, Montine TJ, et al. Diabetes and insulin in regulation of brain cholesterol metabolism. Cell Metab. 2010;12:567-79.
[58] Korade Z, Kenworthy AK. Lipid rafts, cholesterol, and the brain. Neuropharmacology. 2008;55:1265-73.
[59] McDaniel FK, Molden BM, Mohammad S, Baldini G, McPike L, Narducci P, et al. Constitutive cholesterol-dependent endocytosis of melanocortin-4 receptor (MC4R) is essential to maintain receptor responsiveness to alpha-melanocyte-stimulating hormone (alpha-MSH). J Biol Chem. 2012;287:21873-90.
[60] Koza RA, Nikonova L, Hogan J, Rim JS, Mendoza T, Faulk C, et al. Changes in gene expression foreshadow diet-induced obesity in genetically identical mice. PLoS Genet. 2006;2:e81.
[61] Lim WL, Lam SM, Shui G, Mondal A, Ong D, Duan X, et al. Effects of a high-fat, high-cholesterol diet on brain lipid profiles in apolipoprotein E epsilon3 and epsilon4 knock-in mice. Neurobiol Aging. 2013;34:2217-24.
[62] Bryleva EY, Rogers MA, Chang CC, Buen F, Harris BT, Rousselet E, et al. ACAT1 gene ablation increases 24(S)-hydroxycholesterol content in the brain and ameliorates amyloid pathology in mice with AD. Proc Natl Acad Sci U S A. 2010;107:3081-6.
[63] Hutter-Paier B, Huttunen HJ, Puglielli L, Eckman CB, Kim DY, Hofmeister A, et al. The ACAT inhibitor CP-113,818 markedly reduces amyloid pathology in a mouse model of Alzheimer's disease. Neuron. 2004;44:227-38.
[64] Shibuya K, Morikawa S, Miyamoto M, Ogawa SI, Tsunenari Y, Urano Y, et al. Brain Targeting of Acyl-CoA:Cholesterol O-Acyltransferase-1 Inhibitor K-604 via the Intranasal Route Using a Hydroxycarboxylic Acid Solution. ACS Omega. 2019;4:16943-55.

**Figure 1. Non-oral administration of avasimibe decreased body weight and fat weight in DIO mice.**

HF diet-fed 21-26-week-old obese mice (male) were daily treated with vehicle (CTRL) or avasimibe (AVA) (20mg/kg body weight) intraperitoneally (*i.p*) for 13 days. At the end of the study, the mice were sacrificed after overnight fasting for tissue collection and measurements as follows: (**A**) serum alanine transaminase level was determined with associated kits. (**B**) Body weight (n = 9) was measured every other day during the 13 days of treatments. (**C**) The percentage decrease in body weight was calculated relative to the initial body weight. Changes in fat and lean mass were assessed with Dual-energy X-ray absorptiometry. Individual fat pad weight (**E**) and organ weight (**F**) of these DIO mice were measured after euthanization. (**D**). n = 9. *Ing*: inguinal, *Epi*: epididymal, *Retro*: retroperitoneal. All data presented were mean ± S.E.M. *p* values were calculated using Student's t-test. *, $p < 0.05$; **, $p < 0.01$; ***, $p < 0.001$.

**Figure 2. Non-oral administration of avasimibe suppressed food intake and increased energy expenditure.**

Daily food intake (**A**) was measured during the second week of treatment (average of day 6 to day 12) (n = 9). After 13 days of *i.p*. injection of avasimibe (20mg/kg body weight) or vehicle solution, mice (n = 5) were put into the metabolic chamber for detecting $VO_2$ and $VCO_2$ every 22 minutes for 4 days. Average of two dark cycles and two light cycles (21h–

69h) were used to calculate energy expenditure (EE) (**B**) and respiratory exchange ratio (RER) (**C**). The details of the EE (**D**) and the RER (**E**) over time are shown. All data presented were mean ± S.E.M. *p* values were calculated using Student's t-test. *, $p < 0.05$; ***, $p < 0.001$.

**Figure 3. Non-oral administration of avasimibe improved insulin sensitivity and improved serum lipid profile.**

After 3 days of avasimibe (20 mg/kg body weight) *i.p.* injection or vehicle treatment, the DIO mice fasted for 6 h were used for tail blood glucose measurement by a glucometer (**A**) (n = 9). IPGTT was performed in DIO mice after 11 days of avasimibe (20 mg/kg body weight) or vehicle treatment by an *i.p.* injection of glucose at 1.5 g/kg body weight for measurements of blood glucose levels (**B**) and the area under the curve (AUC) (**C**) (n = 9). (**D**) After 13 days of avasimibe (20 mg/kg body weight) *i.p.* injection or vehicle treatment followed by a 4-day of metabolic measurements, the DIO mice fasted overnight were subjected to blood glucose and insulin analyses (n = 9). HOMA-IR (**E**) was calculated as stated in Materials and Methods. The levels of serum FC (**F**), CE (**G**), TG (**H**), and lipolysis-related free glycerol (**I**) and free fatty acids (**J**) were determined by corresponding reagents (n = 9). All data presented were mean ± S.E.M. *p* values were calculated using Student's t-test. *, $p < 0.05$; ***, $p < 0.001$.

**Figure 4. Non-oral administration of avasimibe modulated the leptin production and mRNA levels of adipokine genes and *de novo* lipogenic genes in epiWAT.**

After 13days of *i.p.* injection of avasimibe (20 mg/kg body weight) or vehicle treatment to DIO mice followed by a 4-day of metabolic measurements, overnight fasted mice were subjected to EpiWAT isolation and total RNA extraction to examine the mRNA levels of genes involved in adipogenesis (*PPARγ* and *SREBP1c*), fatty acid synthesis (*ACC*, *FAS* and *SCD1*), TG synthesis (*MGAT1* and *DGAT2*) and cholesterol homeostasis (*SREBP1a*, *SREBP2* and *LDLR*) (**A**), adipokines (*leptin* and *adiponectin*) (**B**), inflammatory cytokines (*MCP1, IL-6, TNFα, CCL5* and *CCL7*), pan-macrophage marker genes (*CD68* and *F4/80*), M2 macrophage marker genes (*MGL2* and *ARG1*), and fibrosis (*TGFb1* and *MMP2*) (**D** and **E**) by real-time PCR analysis (n = 4). Signals were normalized to *RPL27* and *β-actin*. (**C**) Serum leptin levels in these mice were determined by corresponding reagents (n = 9). All data presented were mean ± S.E.M. *p* values were calculated using Student's t-test. *, $p < 0.05$; **, $p < 0.01$; ***, $p < 0.001$.

**Figure 5. The beneficial effect of non-oral administration of avasimibe in weight loss was attributed mainly to the reduction of food intake.**

DIO mice were fasted overnight after 13 days of *i.p.* injection of avasimibe (20 mg/kg body weight) or vehicle treatment followed by a subsequent 4-day of metabolic measurements.

(**A**) The hypothalamus tissues obtained from the mice in CTRL and AVA group (n=3-5/group) were subjected to the analysis for the mRNA levels of genes in appetite control (*NPY, AGRP, POMC, CART* and *MC4R*) and inflammation (*MCP1, TNF$\alpha$* and *IL1$\beta$*) by real-time PCR analysis. Signals were normalized to *$\beta$-actin*. HF diet-fed DIO male mice (29-37 weeks old) treated with *i.p.* injection of avasimibe (AVA, 20 mg/kg body weight) or vehicle (CTRL, Pair) for 8 days under *ad libitum* or pair-feeding regimen were subjected to daily body weight (**B**), changes in body weight (**C**) and food intake (**D**) (n = 4). After five days of avasimibe (20 mg/kg body weight) or vehicle treatment, mice were subjected to respiratory exchange ratio (**E**) and energy expenditure (**F**) measurements (n = 4). Fecal samples from these mice (n = 4) were used for daily fecal excretion (**G**) and fecal energy density (**H**) measurements. All data presented were mean ± S.E.M. *p* values were calculated using Student's t-test. *, $p < 0.05$; **, $p < 0.01$; ***, $p < 0.001$. The data in panels D - H were analyzed via One-way ANOVA with Bonferroni post hoc test. Different letters indicated significant differences.

Figure

Click here to access/download;Figure;Revised figures (FINAL).pptx

# Figure 1

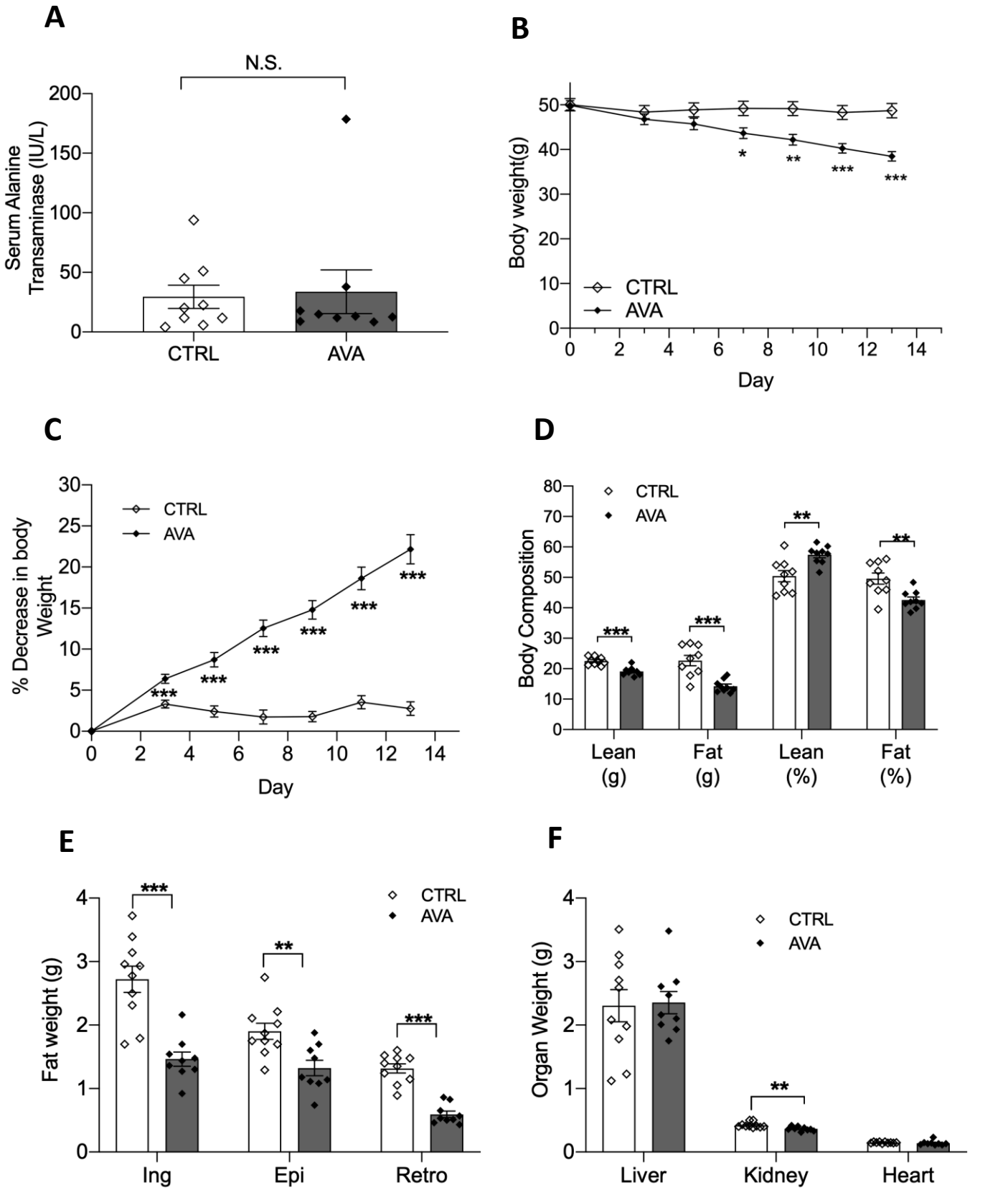

# Figure 2

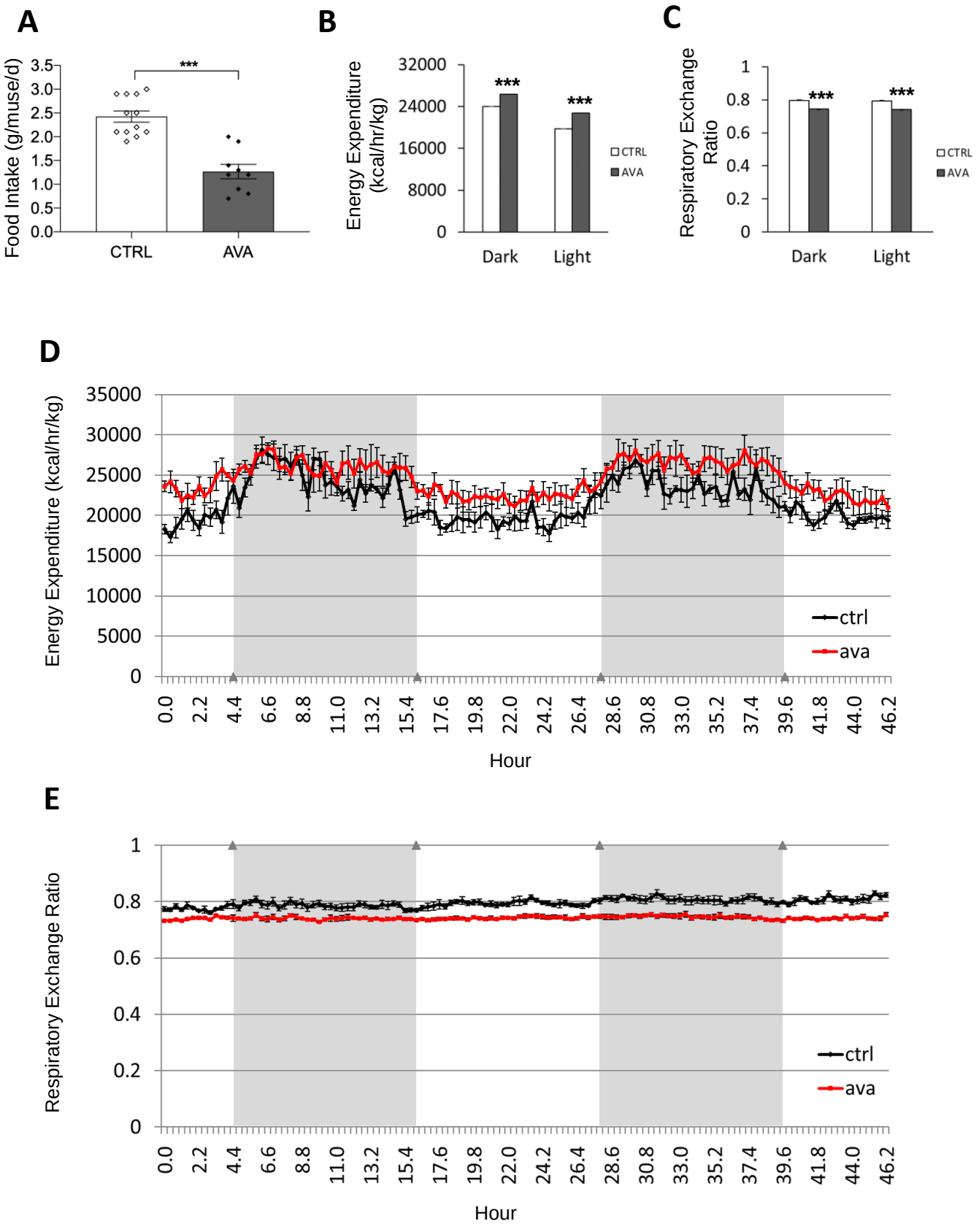
A
Food Intake (g/muse/d)
3.5
3.0
2.5
2.0
1.5
1.0
0.5
0.0
***
CTRL
AVA
B
Energy Expenditure (kcal/hr/kg)
32000
24000
16000
8000
0
***
***
Dark
Light
CTRL
AVA
C
Respiratory Exchange Ratio
1
0.8
0.6
0.4
0.2
0
***
***
Dark
Light
CTRL
AVA
D
Energy Expenditure (kcal/hr/kg)
35000
30000
25000
20000
15000
10000
5000
0
ctrl
ava
0.0
2.2
4.4
6.6
8.8
11.0
13.2
15.4
17.6
19.8
22.0
24.2
26.4
28.6
30.8
33.0
35.2
37.4
39.6
41.8
44.0
46.2
Hour
E
Respiratory Exchange Ratio
1
0.8
0.6
0.4
0.2
0
ctrl
ava
0.0
2.2
4.4
6.6
8.8
11.0
13.2
15.4
17.6
19.8
22.0
24.2
26.4
28.6
30.8
33.0
35.2
37.4
39.6
41.8
44.0
46.2
Hour

# Figure 3

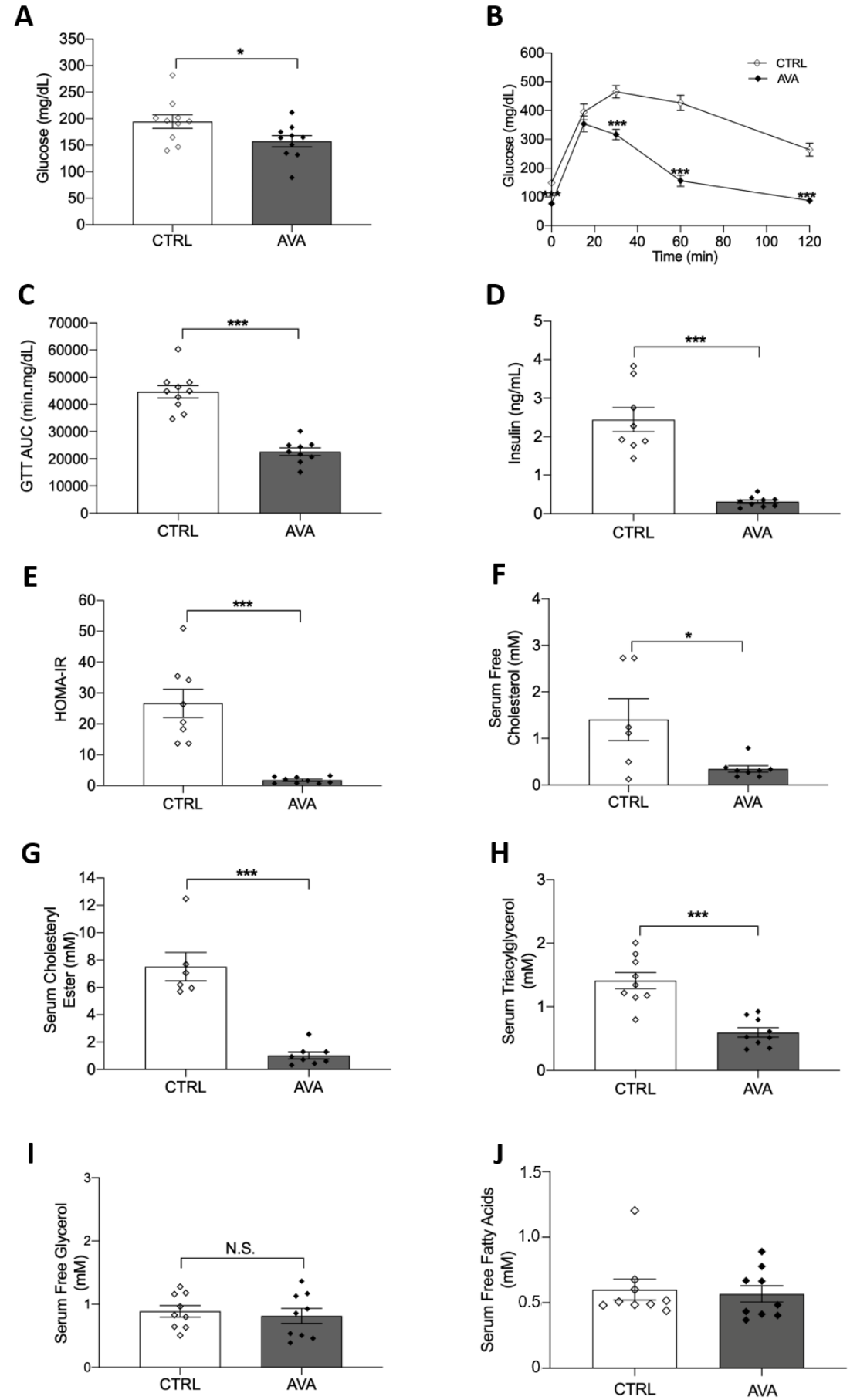
A
Glucose (mg/dL)
350
300
250
200
150
100
50
0
*
CTRL
AVA
B
Glucose (mg/dL)
600
500
400
300
200
100
0
CTRL
AVA
***
***
***
***
0
20
40
60
80
100
120
Time (min)
C
GTT AUC (min.mg/dL)
70000
60000
50000
40000
30000
20000
10000
0
***
CTRL
AVA
D
Insulin (ng/mL)
5
4
3
2
1
0
***
CTRL
AVA
E
HOMA-IR
60
50
40
30
20
10
0
***
CTRL
AVA
F
Serum Free Cholesterol (mM)
4
3
2
1
0
*
CTRL
AVA
G
Serum Cholesteryl Ester (mM)
14
12
10
8
6
4
2
0
***
CTRL
AVA
H
Serum Triacylglycerol (mM)
3
2
1
0
***
CTRL
AVA
I
Serum Free Glycerol (mM)
3
2
1
0
N.S.
CTRL
AVA
J
Serum Free Fatty Acids (mM)
1.5
1.0
0.5
0
CTRL
AVA

# Figure 4

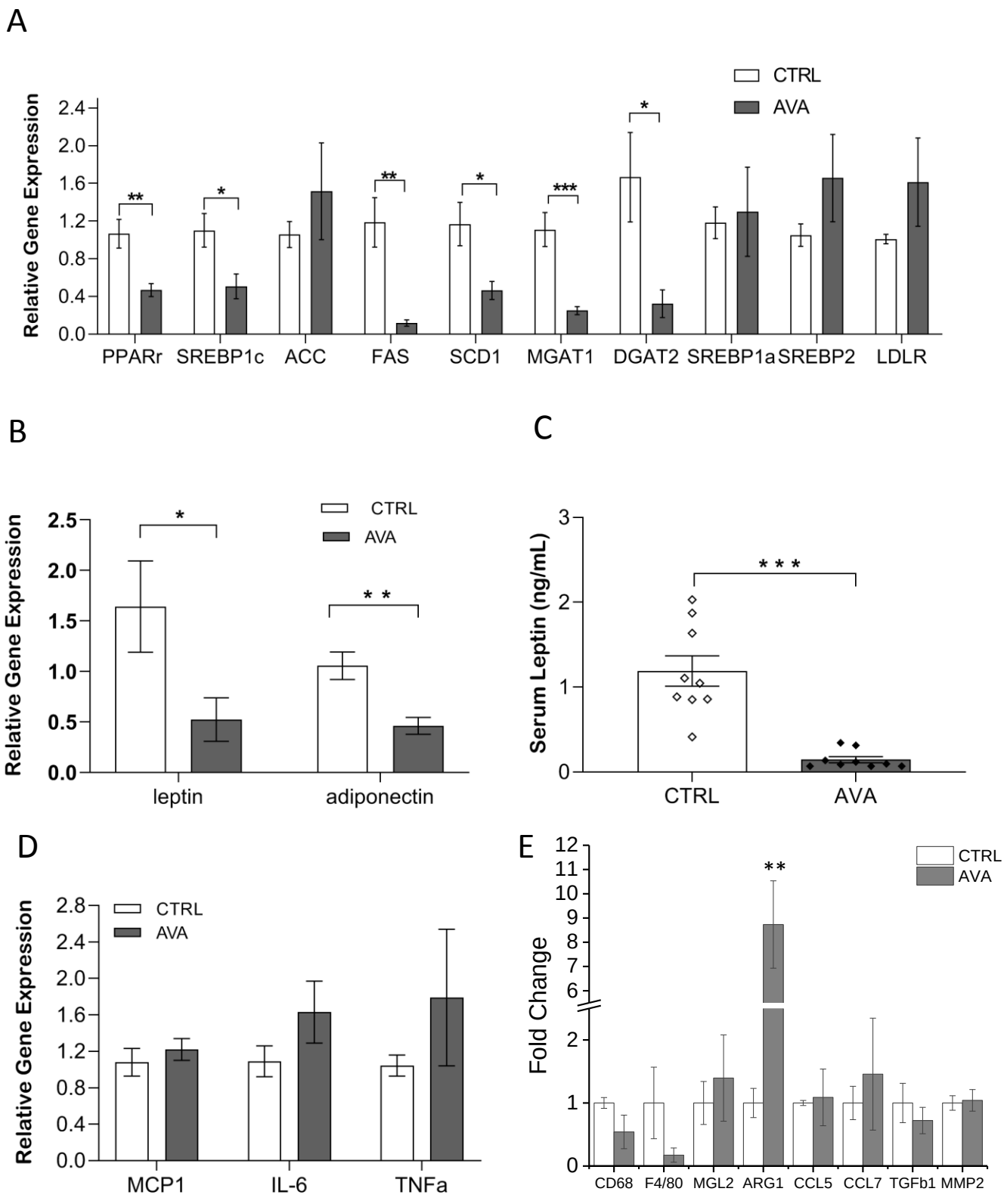
A
CTRL
AVA
Relative Gene Expression
2.4
2.0
1.6
1.2
0.8
0.4
0.0
**
*
**
*
***
*
PPARr
SREBP1c
ACC
FAS
SCD1
MGAT1
DGAT2
SREBP1a
SREBP2
LDLR
B
CTRL
AVA
Relative Gene Expression
2.5
2.0
1.5
1.0
0.5
0.0
*
* *
leptin
adiponectin
C
Serum Leptin (ng/mL)
3
2
1
0
* * *
CTRL
AVA
D
CTRL
AVA
Relative Gene Expression
2.8
2.4
2.0
1.6
1.2
0.8
0.4
0.0
MCP1
IL-6
TNFa
E
CTRL
AVA
Fold Change
12
11
10
9
8
7
6
2
1
0
**
CD68
F4/80
MGL2
ARG1
CCL5
CCL7
TGFb1
MMP2

# Figure 5

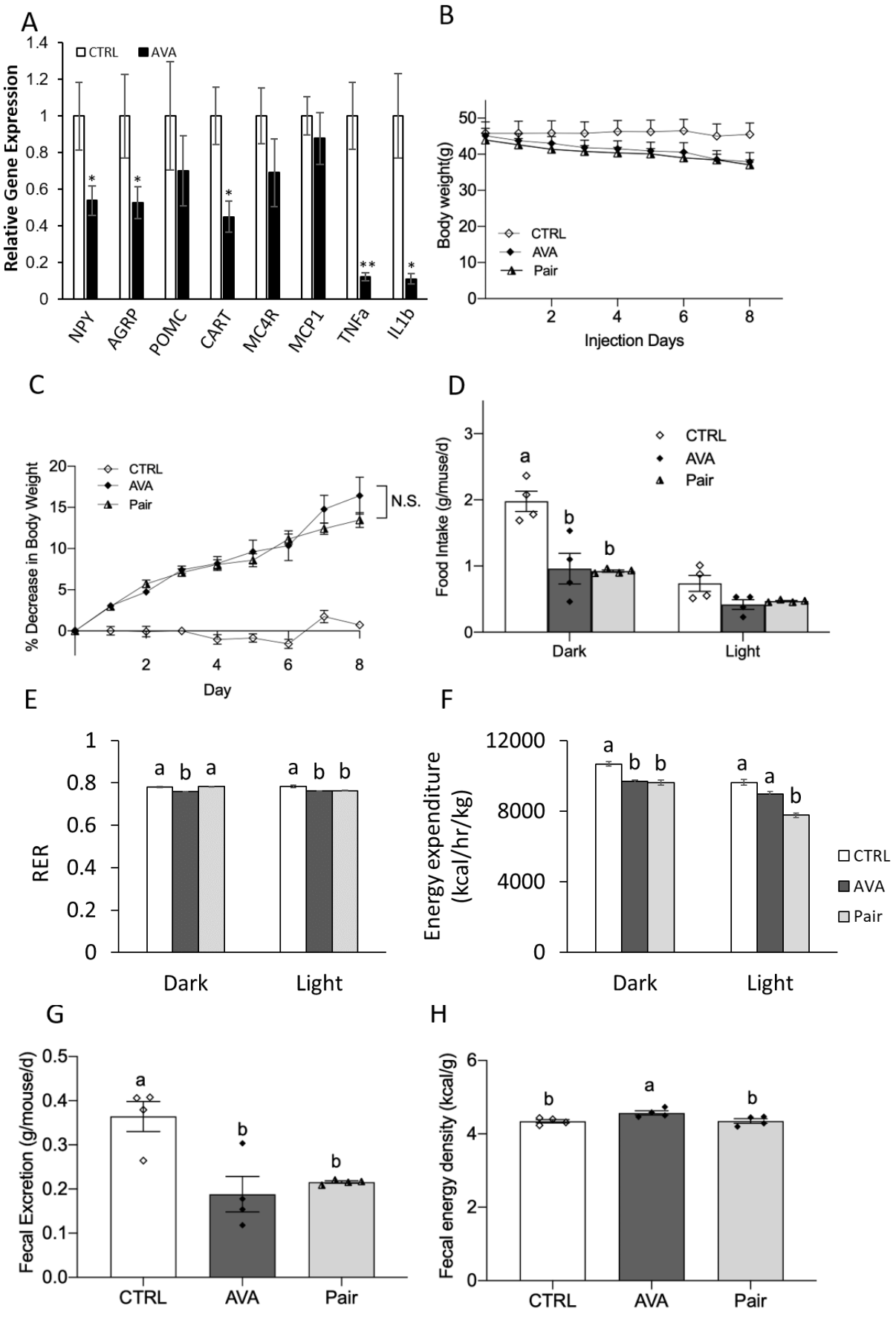
A
CTRL
AVA
Relative Gene Expression
NPY
AGRP
POMC
CART
MC4R
MCP1
TNFa
IL1b
B
Body weight(g)
CTRL
AVA
Pair
Injection Days
C
% Decrease in Body Weight
CTRL
AVA
Pair
N.S.
Day
D
Food Intake (g/muse/d)
CTRL
AVA
Pair
Dark
Light
E
RER
Dark
Light
F
Energy expenditure (kcal/hr/kg)
CTRL
AVA
Pair
Dark
Light
G
Fecal Excretion (g/mouse/d)
CTRL
AVA
Pair
H
Fecal energy density (kcal/g)
CTRL
AVA
Pair

with SAS 9.2 (SAS® Inst. Inc., Cary, NC). A *P*-value of less than 0.05 was considered statistically significant.

**8. Experimental animals**

Six to eight-week-old male C57BL/6J mice (The Jackson Laboratory, Bar harbor, ME) were fed with high-fat (HF) diet (60% of calories from fat) (cat. no. TD.06414, Harlan Laboratories, Madison, WI) for 15 - 20 weeks to develop diet-induced obesity. These diet-induced obese (DIO) mice were then randomly assigned to control (CTRL) and avasimibe (AVA) groups. The mice were kept on a 12/12 h light/dark cycle at 22 - 25°C, with HF diet and water *ad libitum*. Experimental procedures were approved by the Purdue University Institutional Animal Care and Use Committee (protocol no. 1112000347).

**9. Experimental procedures**

Avasimibe was dissolved in vehicle solution (avasimibe first dissolved in dimethyl sulfoxide (DMSO) at a concentration of 90mg/ml, then diluted with 2-hydroxypropyl-β-cyclodextrin and Tween-80 in PBS, making the final concentration of avasimibe at 2.7mg/ml, DMSO at 3% (v/v), tween-80 at 2% (v/v) and 2-hydroxypropyl-β-cyclodextrin at 3.2mg/ml. We injected avasimibe solution or vehicle at 7.7ul /g body weight, corresponding to 20 mg/kg body weight, to the mice in the AVA and CTRL groups intraperitoneally (*i.p*.) daily for indicated days. Food and body weight were determined every other day or daily.

DIO C57BL/6J mice (male, 29-37 weeks of age) were randomly assigned to CTRL, AVA and pair-feeding (Pair) groups. Mice from the AVA group received a 20 mg/kg body weight dosage of avasimibe through daily *i.p*. injection, while mice from the CTRL and PAIR groups received vehicle solution. Food intake of these mice was measured twice daily, at the beginning of the light and dark cycles. Thus, the food consumption during the light cycle was calculated by (food amount in the cage at 7 am – food amount in the cage at 7 pm). Food consumption during the dark cycle was calculated by (food amount in the cage at 7 pm – food amount in the cage at 7 am the next day). The restricted-food administration of Pair group was staggered one day later than the treatment of CTRL and AVA groups. All the Pair mice were given the same amount of food consumed by the AVA mice on the previous day. The mice in the CTRL and AVA groups were allowed to access the HF diet *ad libitum*. All the mice used in this study were allowed to access water *ad libitum.* Body weight was monitored every day. At the end of the treatments, mice were subjected to the physiological, biochemical and molecular assays described in the Material and Method section.

**10. Results**

**Author Statement**

Zhu, Y. designed and analyzed the research, performed all the experiments, and wrote the manuscript. Kim, K.-H. designed, analyzed, and supervised the research and wrote the manuscript. Kim, S.Q., Zhang Y. and Liu, Q. analyzed data and prepared the manuscript. The manuscript was critically reviewed and approved by all authors.